Self-Assembly of Methyl Zinc (3^1R)- and (3^1S)-Bacteriopheophorbides *d*

Teodor Silviu Balaban,[†] Hitoshi Tamiaki,[‡] Alfred R. Holzwarth,*[,†] and Kurt Schaffner[†]

Max-Planck-Institut für Strahlenchemie, Postfach 10 13 65, D-45413 Mülheim an der Ruhr, Federal Republic of Germany, and Department of Bioscience and Biotechnology, Faculty of Science and Engineering, Ritsumeikan University, Kusatsu, Shiga 525-77, Japan

Received: September 19, 1996; In Final Form: December 13, 1996[⊗]

The methyl zinc (3^1R)- and (3^1S)-[8Et,12Me]bacteriopheophorbides d—analogs of the light-harvesting bacteriochlorophylls in photosynthetic bacteria—self-assemble in nonpolar solvents. While in dilute dichloromethane solution both epimers prevail in their monomeric form, complex equilibria of aggregates with gradually red-shifting Q_y absorptions are formed at either higher concentration or lower temperature or upon dilution with hexane. Dynamic ^{1}H-NMR and FT-IR spectroscopies show that the 3^1-hydroxy group participates directly in the self-assembly through oxygen ligation to zinc and through hydrogen bridging to the 13^1-keto group of the ligated hydroxyls in intermediate unsymmetrical dimers. The basic unit, combining three molecules through >C═O···H−O···Zn bonding, and the existence of equilibria between monomers, dimers, and oligomers of varying size depending on the conditions parallel the scheme proposed previously for bacteriochlorophylls *c* and *d* (Chiefari, J.; et al. *J. Phys. Chem.* **1995**, *99*, 1357−1365. Holzwarth, A. R.; Schaffner, K. *Photosynth. Res.* **1994**, *41*, 225−233). In some respects the CD, ^{1}H-NMR, and IR spectral behavior of the two epimers indicates diastereoselective conformational and kinetic differences at the levels of dimers and larger oligomers. *Inter alia*, the self-assembly of a 1:1 mixture of the (3^1R) and (3^1S) epimers proceeds more rapidly than that of the separate epimers. This is possibly of relevance with regard to the rodlike aggregates in the interior of the chlorosomes of certain bacterial species which are composed of both 3^1-epimeric bacteriochlorophylls.

Introduction

Molecular self-assembly to form supramolecular systems is presently a topic of acute interest concerning both fundamental and practical aspects in life and materials sciences. In photosynthetic antennae a large number of chromophores are associated in light-harvesting complexes, which function by capturing radiant energy and transmitting it to the reaction center, where it is converted into chemical energy. While most commonly the chromophores are embedded in protein matrices,[1] another type of antenna complex is encountered in green photosynthetic bacteria.[2] In the so-called chlorosomes pigment−pigment interactions predominate within large aggregates of bacteriochlorophyll(BChl)s *c* and *d* assembled by noncovalent binding,[3] thus providing for synthetic and genetic economy in the generation of a supramolecular system[4] and adding another key function to those performed in nature by self-assemblies, such as base pair recognition and antibody−antigen interaction.

Since large aggregates of the type encountered in the hydrophobic environment of the chlorosome interior are also accessible by self-assembly of either natural BChls *c* and *d* or synthetically more readily available model chlorins *in vitro* in hexane solution,[5] we have concentrated on studying the mechanism of formation and supramolecular structure of such aggregates and the structural constraints of the monomers involved. A purpose beyond the phenomenological elucidation is to explore the self-organization of this complex supramolecular system toward applicatory exploitation of the structural principle in the field of photoactive supramolecular devices.[6] We have recently reported[7] how the self-assembly of synthetic chlorins possessing the appropriate electronic energy donor and acceptor sites can lead to a photophysically functioning artificial unit.

The absorption spectra of the chlorosomes and of the aggregates of BChls and magnesium-containing synthetic analogs in nonpolar solvents are quite similar, all red shifted by as much as 70 nm with respect to monomeric BChl in polar solvents. When the magnesium atom is replaced by zinc, the self-assembly capability is maintained, only the absorption is blue shifted by 10 nm for the monomers (in polar solvents) and by about 20 nm for the aggregates (in nonpolar solvents). Extensive studies by vis absorption,[8] FT-IR,[8] resonance Raman,[9] and solid-state NMR spectroscopies[10] have shown that at least all proximal interactions in the chlorosomes and in the self-assembled large BChl and model chlorin aggregates are the same. The essential functions for the self-assembly process are the central metal atom and the 3^1-hydroxy and 13^1-keto groups.[11] Experimental data[8,9b] and molecular modeling[12] show that the linkage between the individual chlorins in a large aggregate is accomplished by the 3^1-hydroxy group of one chlorin bridging the metal atom of another chlorin with the 13^1-keto group of a third chlorin, >C═O···H−O···M(═Mg, Zn).[13] The extension of this bonding unit to a supramolecular network results in a three-dimensional tubular structure.[12a,14]

The 3^1-hydroxy group assumes a central role in this cooperative interaction between the aggregated molecules. Accordingly, its stereochemistry plays an important part in determining the nature of the self-assembled structures.[8,19−21] In this contribution we describe the detailed spectroscopic study of the self-assembly of two 3^1-epimers of a methyl zinc bacteriopheophorbide *d*(**1**).[19] It constitutes a continuation and extension of our earlier papers on the aggregation of magnesium-containing BChl *c*.[8,18] The advantages of working with zinc analogs of the BChls are greater chemical stability and a more facile synthetic access, both factors of which have been exploited in our experimental approach to chlorosome modeling.[7,11,20] The relevance for naturally occurring light-harvesting systems is highlighted by

[†] Max-Planck-Institut für Strahlenchemie.
[‡] Ritsumeikan University.
[⊗] Abstract published in *Advance ACS Abstracts,* April 1, 1997.

S1089-5647(96)02872-6 CCC: $14.00

the recent discovery of a zinc-containing BChl in an aerobic photosynthetic bacterium.[22] Furthermore the conclusions drawn herein on the Zn compounds can be extrapolated to the BChls *c*, *d*, and *e* having a 3^1-hydroxy group of corresponding chirality.

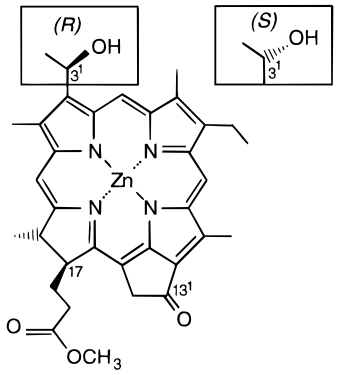

1

Experimental Section

Solvents were of spectroscopic grade and were used without further purification.

UV−vis spectra were recorded either on a Shimadzu UV-2102 PC scanning spectrophotometer or on an Omega 1-Bruins Instruments spectrophotometer equipped with an Oxford Instruments cryostat and a PT100 thermocouple. FT-IR spectra were measured on a Bruker IFS66 FT-IR spectrophotometer in CaF_2 cells of 0.5-mm pathlength. The neat solvent served as a reference. Low-temperature FT-IR spectra were recorded in a 1-mm CaF_2 cell mounted on an in-house-built cryostat. CD spectra were run either on an Aviv CD spectrometer, Model 62A DS, also equipped with an Oxford Instruments cryostat, or on a Jasco J20 instrument. ^{1}H-NMR spectra were recorded at 400 MHz in CD_2Cl_2 on a Bruker AM 400 spectrometer equipped with the variable-temperature unit.

The methyl zinc (3^1R)- and (3^1S)-bacteriopheophorbides **1** were prepared according to the literature.[19] The epimers were then separated by HPLC on a Nucleosil 7C18 column (250 × 20 mm; Machery-Nagel) with methanol/water (5:1 v/v, 5 mL/min; λ_{obs} 460 nm; (3^1R), 25 min; (3^1S), 28.5 min). The two fractions were concentrated *in vacuo*, and the residues were taken up in CH_2Cl_2. The solutions were washed three times with brine, dried over Na_2SO_4, and then concentrated *in vacuo*.

Results

Visible Absorption. Figures 1 and 2 show the concentration and temperature dependences, respectively, of the vis absorption of the two epimers of **1** in CH_2Cl_2. The temperature changes are fully reversible. Both the increase in concentration and the lowering in temperature favor aggregation, which is indicated by a red shift of the absorption maxima. We presume that each component of the self-assembly equilibrium possesses its own distinct absorption spectrum and that the red shift is qualitatively correlated to the size of the species.

At room temperature and concentrations < 0.05 mM both epimers have a sharp Q_y maximum (fwhm = 27 nm) at 649 nm (3^1R) and 648 nm (3^1S). These maxima are those of the monomers, since they are also obtained in polar solvents (diethyl ether, tetrahydrofuran, methanol) and by addition of methanol to CH_2Cl_2 solutions.

It is evident from Figures 1 and 2 that (3^1R)- and (3^1S)-**1** behave differently in aggregation. As the concentration of (3^1R)-**1** is increased, a shoulder grows in at 660 nm, gradually

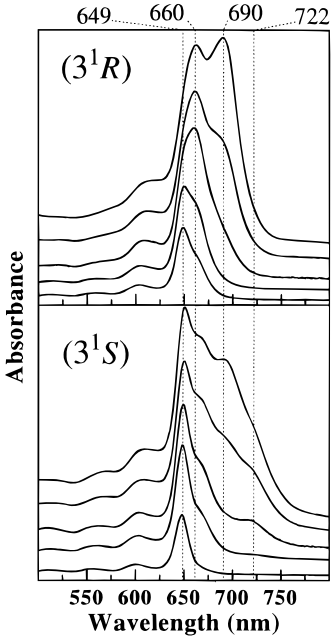

Figure 1. Concentration dependence of the vis absorption of (3^1R)- and (3^1S)-**1** in CH_2Cl_2 at room temperature. Concentrations (mM) from top to bottom: (3^1R), 6.88, 3.10, 1.38, 0.33, 0.14; (3^1S), 5.0, 2.5, 1.0, 0.55, 0.28, 0.08. The three traces with the greatest concentrations were recorded in a 0.01-cm quartz cuvette, the others in 0.1-cm cuvettes. The concentrations were determined by weighing; the precision for the most concentrated samples is ±0.15 mM. Note that different scaling factors have been used for the individual absorbances.

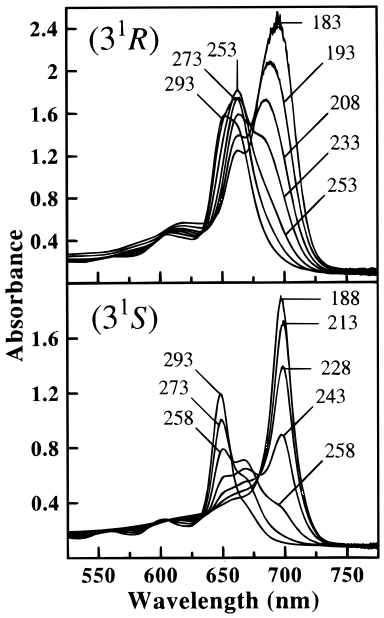

Figure 2. Temperature dependence of the vis absorption of (3^1R)- and (3^1S)-**1** in CH_2Cl_2. The temperatures are given in K (±2); the concentrations are 0.5 mM for (3^1R)-**1** and 0.3 mM for (3^1S)-**1**. The 0.1-cm quartz cuvette was not removed from the spectrophotometer while the cryostat was being cooled.

substituting the monomer band and shifting the maximum from 649 to 659 nm at 1.38 mM. We ascribe this latter maximum to a dimer. At still higher concentrations, another shoulder appears at 690 nm and increases to a distinct new 690.5-nm maximum in nearly saturated solutions. This new band is assigned to a tetramer which arises from two dimers joining since the relative monomer concentration has concomitantly decreased to a considerable extent. The situation with the (3^1S) epimer is different. Three red-shifted shoulders (at 666, 690,

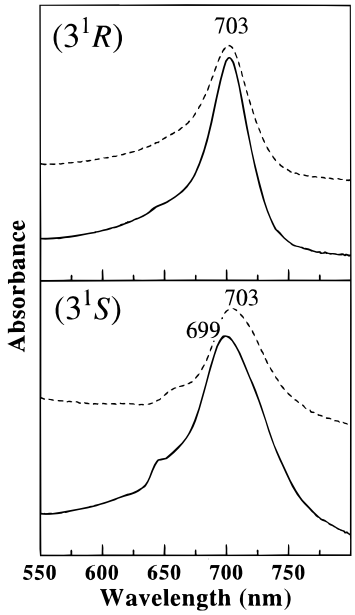

Figure 3. Vis absorption spectra of **1** in CH_2Cl_2 solution (ca. 5 mmol/L) that had been diluted with hexane (5:95 v/v) (—) and in a film on the cuvette wall deposited from a more dilute CH_2Cl_2 solution after dilution with hexane and decanting the supranatant (- - -). Note that the absorbance scale of the films is expanded by a factor of 10 over that of the corresponding solutions.

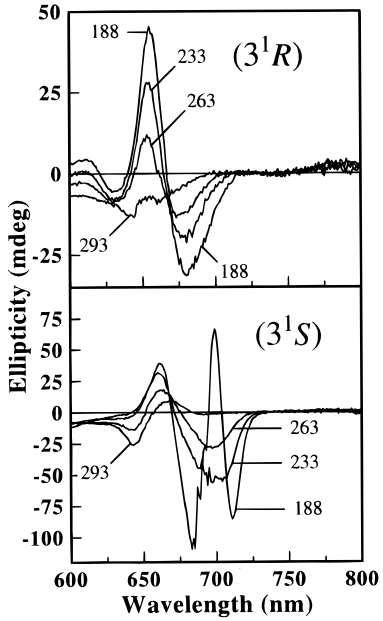

Figure 4. CD Spectra of (3^1R)- and (3^1S)-**1** in CH_2Cl_2 at different temperatures (given in K). The concentrations were 0.47 mmol/L for (3^1R) and 0.46 mmol/L for (3^1S); the path length was 0.1 cm.

and 722 nm) appended to the monomer maximum appear with increasing concentration. It is of interest to note that the 722-nm shoulder appears prior to, *i.e.* already at a lower concentration than, the one at 690 nm, but at >1.0 mM it is bypassed in intensity by the 690-nm absorption.

A dimerization constant, K_d, cannot be determined accurately because the absorption coefficients of the dimers and the monomers probably differ. However, it is clear that K_d is larger for (3^1R)-**1** than for (3^1S)-**1**, the monomeric form of which is present to a considerably greater extent even in highly concentrated solutions (see Figure 1).

Upon cooling, the equilibria among the (3^1R) species are shifted first toward the dimers (at 660 nm), which predominate between 273 and 253 K, and then toward the tetramers absorbing at 690 nm (Figure 2). In the case of (3^1S)-**1**, the monomer peak at 648 nm gradually decreases with temperature, and an intermediate form absorbing at about 666 nm grows in at 258 K. Upon further cooling, a new sharp band at 696 nm appears to be formed at the cost of both the 649- and 666-nm species. The 722-nm form, present in the concentrated solutions at room temperature, does not appear at lower temperatures. In summary, (i) below 193 K dimers are more abundant in the case of (3^1R)-**1** than (3^1S) (this will be important when evaluating the low-temperature NMR data; see below), (ii) at low temperature the fwhm of the main band is 39 nm for (3^1R) and only 19 nm for (3^1S), indicating a much more homogeneous distribution of aggregate species in the latter case, and (iii) the band area significantly increases upon cooling, indicating a gain in oscillator strength so that again no relationship appears to exist between the absorption coefficients of the equilibrium components.

When a concentrated CH_2Cl_2 solution of either epimer is diluted at room temperature with a nonpolar solvent such as hexane, the maxima are red shifted to 705 nm for (3^1R) and 700 nm for (3^1S) (Figure 3). We have shown that this is an autocatalytic process.[18] The peak of (3^1S)-**1** is asymmetric and significantly broader (fwhm = 61 nm) than the (3^1R) band (fwhm = 37 nm). Also the shoulder at 650 nm is more pronounced for (3^1S), indicating that more monomers are present in this latter equilibrium.

From dilute CH_2Cl_2 solutions a thin film is gradually deposited on the walls of the quartz cuvette. The absorption spectra of these films (Figure 3) are quite similar to the aggregate spectra of the hexane solutions. At higher concentrations in CH_2Cl_2 precipitates are formed instead upon standing, and the intensity of red-shifted Q_y absorption maxima is diminished in the supernatants. The precipitates redissolve on vigorous shaking of the cuvette, and the absorptions are intensified again. This behavior parallels the observations already made with BChl *c*.[18]

The aggregates formed upon dilution with hexane exhibit different absorption maxima, however, and therefore should have different supramolecular structures from those formed in CH_2Cl_2 at low temperature. This is especially evident from the CD spectra (see below).

CD Spectra. The influence of temperature on the CD of both epimers in CH_2Cl_2 is illustrated in Figure 4. Multiple Cotton effects appear upon lowering of the temperature. For (3^1R)-**1** a distinct couplet, with a peak at 658 nm and a trough at 680 nm, grows in. Although the rotational strengths are different (the positive Cotton effect is more intense), the positive and negative band areas are almost equal, which indicates that excitonic coupling may be at the origin of these effects. (3^1S)-**1** exhibits a similar spectral behavior at moderately low temperatures, with the peak intensity increasing at 660 nm and a trough developing at 690 nm. However, at −85 °C a new sharp excitonic couplet of considerable intensity appears (peak at 700 nm and trough at 710 nm). This new signal correlates with the sharp absorption bands encountered in CH_2Cl_2 at low temperature (Figure 2).

Completely different CD spectra are obtained when CH_2Cl_2 stock solutions of the two epimers are diluted with hexane or cyclohexane (Figure 5). This implies that the species formed at low temperature in CH_2Cl_2 are different from those generated by dilution with hexane. Another noteworthy feature is the much stronger negative Cotton effect of (3^1S)-**1** at around 725 nm. It correlates with the vis absorption band which is strikingly broad, evidently due to larger oligomers contributing in this

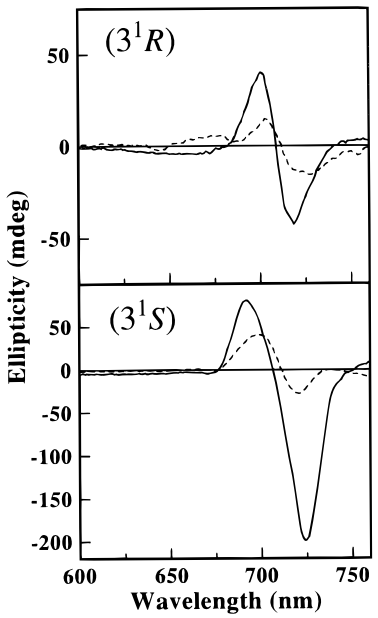

Figure 5. CD spectra of (3¹*R*)- and (3¹*S*)-**1** at room temperature when CH_2Cl_2 stock solutions are diluted with (—) cyclohexane and (- - -) hexane to 5:95 v/v. The final concentrations were 15 μM (3¹*R*)-**1** in cyclohexane and 10 μM (3¹*R*)-**1** in hexane, and 22 μM (3¹*S*)-**1** in cyclohexane and 10 μM (3¹*S*)-**1** in hexane; the path length was 1 cm. In the hexane solutions some green precipitates were deposited during the ca. 40-min duration of the measurements.

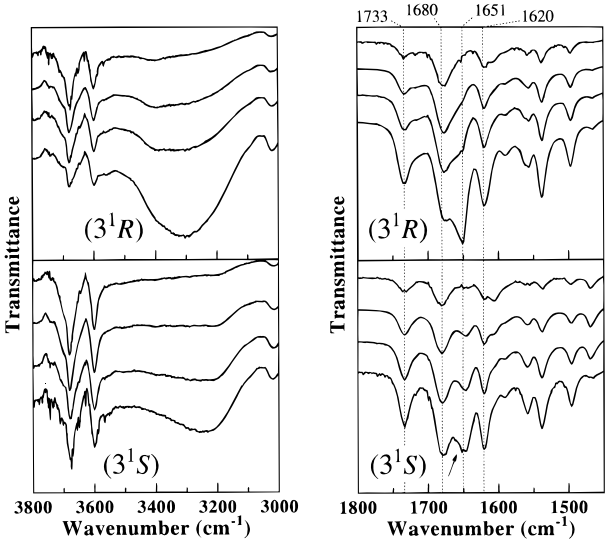

Figure 6. FT-IR spectra of (3¹*R*)- and (3¹*S*)-**1** in CH_2Cl_2 at room temperature and different concentrations. (3¹*R*) (from top trace to bottom): 1.0, 1.9, 2.7, and 5.4 mM. (3¹*S*): 0.6, 1.2, 1.8, and 3.7 mM. Spectra were measured in a CaF_2 cell of 0.5 mm path length. In the trace of (3¹*S*) at 3.7 mM the satellite peak at 1650 cm^{-1} (arrow) is attributed to noise, and the bands of (3¹*R*) and (3¹*S*) at $\geq$3600 cm^{-1} are attributed to water (see ref 8). The transmittance of all traces on the left-hand side (3000−3800 cm^{-1}) is expanded by a factor of 5 relative to that on the right.

wavelength region (Figure 3), such as the 722-nm form noted also in the concentration-dependent absorption spectra (Figure 1).

FT-IR Spectra. Two spectral domains are of special interest, namely, the ν_{OH} region between 3200 and 3500 cm^{-1} and the 1550−1750 cm^{-1} region for carbonyl and chlorin modes. In Figure 6 one notes broad features between 3150 and 3450 cm^{-1} at high concentrations of both (3¹*R*)- and (3¹*S*)-**1**, which correlate with bands growing in at 1651 and 1647 cm^{-1}, respectively, and which evidently indicate a diastereoselective control of the

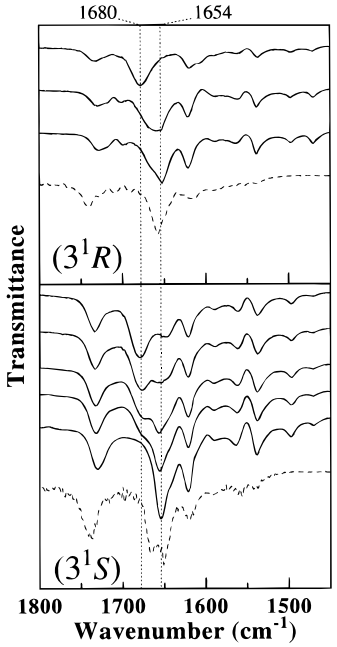

Figure 7. FT-IR spectra of (3¹*R*)- and (3¹*S*)-**1**. (—) In CH_2Cl_2 at different temperatures. Temperatures (from top to bottom) and concentration for (3¹*R*): 293, 223, and 183 K, 1.0 mM. For (3¹*S*): 293, 283, 273, 263, and 203 K, 1.8 mM. (- - -) In hexane at room temperature, ca. 10 μM; the spectra shown are the average of four experimental spectra.

aggregation process. In both epimers at low concentration, where according to the vis absorption spectra only monomers and dimers coexist, the ketone band appears at 1680 cm^{-1}. This implies that in the dimers the ketone is not involved in any intermolecular interactions. As aggregation proceeds to higher concentrations, the ketone carbonyl frequency is lowered concomitantly with the growth of the low-frequency hydroxyl bands owing to participation in ketone-to-hydroxyl hydrogen bridging. It is important to note, also, that the ester carbonyl frequency of 1733 cm^{-1} is not at all affected by concentration, which excludes any participation of this group in intermolecular bonding. Furthermore, the sharp band of the chlorin IR1 mode[23] at 1620 cm^{-1} of both (3¹*R*)- and (3¹*S*)-**1** shows that the 5-coordination of zinc is maintained[11b] throughout the aggregation process.

When CH_2Cl_2 stock solutions of (3¹*R*)-**1** were diluted with hexane, only a strongly hydrogen-bonded ketone band at 1657 cm^{-1} appears, and none of the 1680-cm^{-1} feature. This is illustrated by the 10 μM spectrum in Figure 7. The ester carbonyl band is concomitantly shifted to 1739 cm^{-1}, an only insignificantly higher frequency than in CH_2Cl_2. Under the same conditions, the spectrum of the (3¹*S*) epimer in hexane exhibits a ketone band at 1650 cm^{-1} with a shoulder at 1660 cm^{-1}, besides the band for the ester and the chlorin mode.

The broad features in the OH region appear also at lower temperatures, especially at high concentrations (not shown). This is accompanied in both epimers by a clear shift of the ketone carbonyl frequency from 1680 to 1654 cm^{-1}, either upon cooling from 293 to 183 K or upon dilution with hexane (Figure 7). At room temperature (Figure 6) both bands reach about equal intensities at high concentration. All spectral changes with temperature are fully reversible. The observations are in accord with the spectral changes in vis absorption and in CD with temperature and concentration, which have clearly shown that the hydrogen-bonded species existing at low temperature and at high concentration are different.

It should be noted also that the ester carbonyl frequency of 1732 cm^{-1} again is not at all affected by concentration and

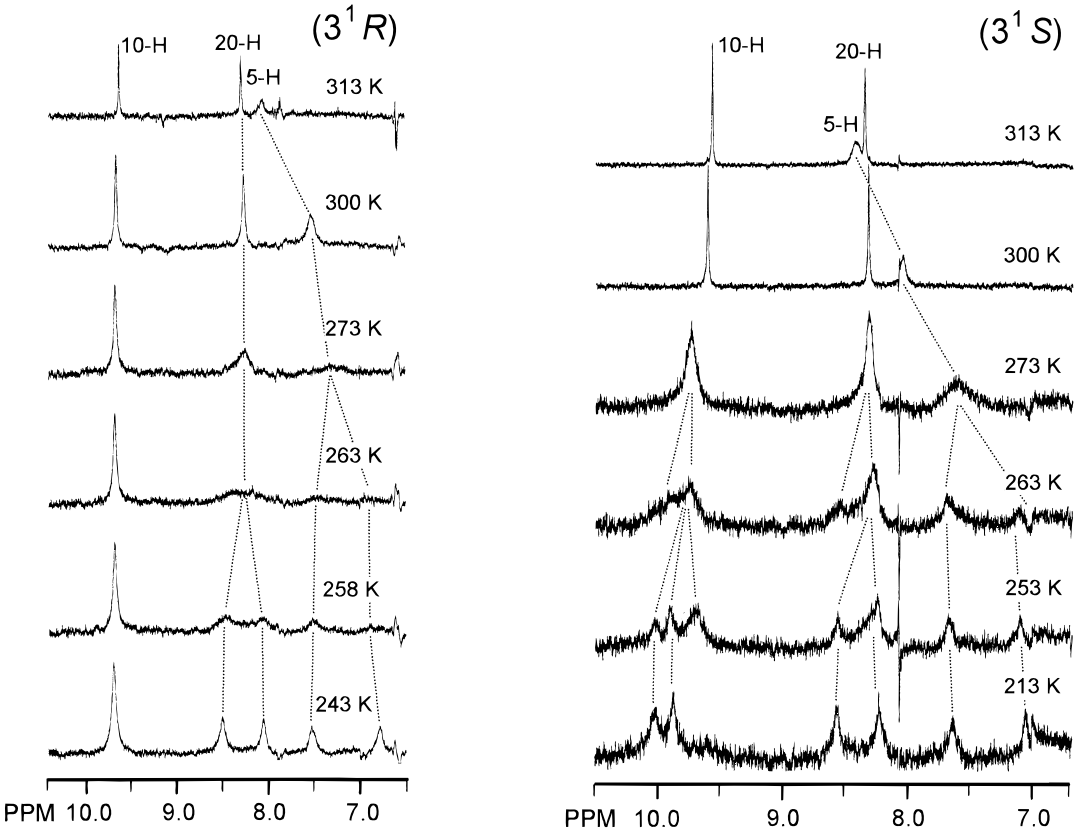

Figure 8. Low-field portion of the 400-MHz ^{1}H-NMR spectra of (3^1*R*)- and (3^1*S*)-**1** in CD_2Cl_2 at different temperatures; concentrations ca. 4 and 2 mM, respectively (cf. the concentration dependence of the vis absorption in Figure 1).

merely a shift of 3 cm^{-1} to lower frequencies is encountered upon cooling, which excludes any participation of this group in the intermolecular bonding.

^{1}H-NMR Spectra. The line width of the C-5 proton proved strongly dependent on the magnetic field strength, which is indicative of a dynamic process and has prompted us to investigate (3^1*R*)- and (3^1*S*)-**1** by variable-temperature NMR in CD_2Cl_2. The room-temperature spectrum of (3^1*R*)-BChl *d* in $CDCl_3$ has been interpreted[24] in terms of either of two nonsymmetrical arrangements of a closed dimer[25] as the predominant species. The structural assignment was based on calculations of ring current shifts. In the investigation of **1** the somewhat different dimer geometries caused by the (3^1*R*)- and (3^1*S*)-hydroxy-to-metal ligation of the respective epimers could be expected to be detectable by ^{1}H-NMR. The spectrum of (3^1*R*)-BChl *d* was reported,[24] furthermore, to exhibit complex signal splitting, indicating that the monomer−dimer equilibrium is within the slow-exchange range at room temperature and 500 MHz. In contrast, Figure 8 shows that the zinc analogs at room temperature and 400 MHz exhibit only one set of signals for each nonequivalent proton due to rapid exchange. Upon cooling, the signals quite generally first shift, indicating a displacement of the monomer−dimer equilibrium toward the dimer, then in part coalesce, and eventually emerge as doublets of equal intensities. This is direct evidence, as in the case of BChl *d*,[24] in favor of a nonsymmetrical dimer conformation for both epimers, as exemplified for (3^1*R*) in Figure 9.[26]

In detail, the spectra of the two epimers exhibit different behaviors (Figure 8). While the C-10 proton signal of (3^1*R*)-**1** remains sharp throughout the temperature range, the corresponding signal of (3^1*S*) is split. This indicates that in the (3^1*R*) dimer the C-10 protons of both halves experience approximately the same magnetic environment, as opposed to the (3^1*S*) epimer. The maintainance of a 1:1 intensity ratio for the split signals

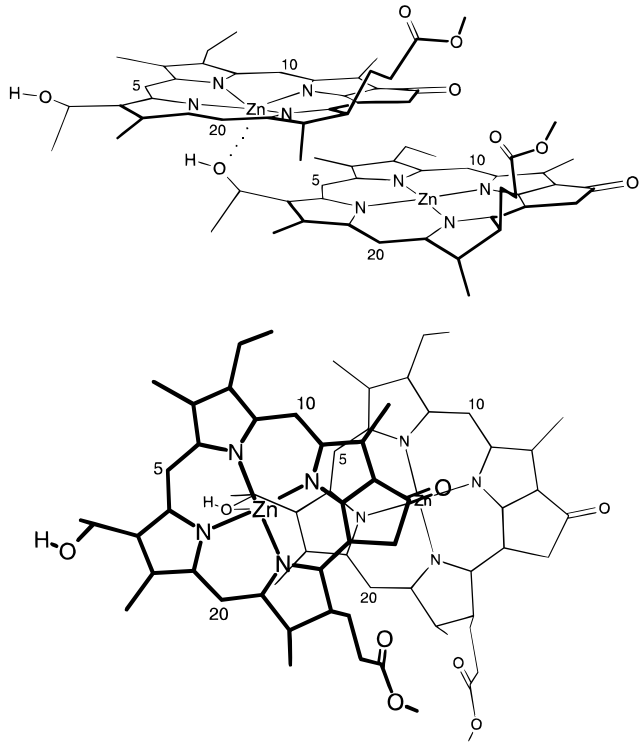

Figure 9. Nonsymmetrical conformation of the open dimer of (3^1*R*)-**1** as deduced from variable-temperature NMR (cf. Figure 8), viewed (top) sideways and (bottom) from above. Double bonds are omitted.

throughout is best compatible with the two dimer halves possessing nonequivalent sites.

The coalescence temperatures of the C-5 proton, which are the ones most readily to be determined, are 268 K for both the (3^1*R*)- and (3^1*S*)-**1** dimers within the error limits of ±1° and

SCHEME 1: Species Involved in the Aggregation−Deaggregation Equilibria,[17,28] Controlled by Concentration, Temperature, and Solvent Nature

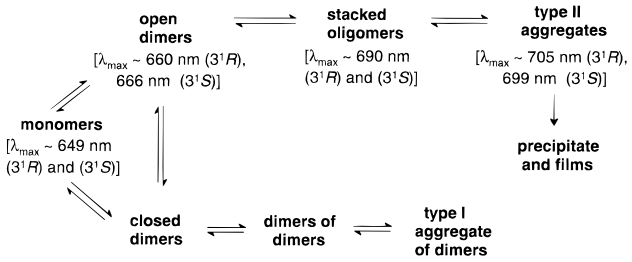

±3°, respectively, with $\Delta G^{\ddagger}_c$ values of 51 kJ. The activation barriers between the two conformational arrangements of each epimer are thus essentially identical. They are only slightly higher—at 268 K—than the dissociation energy of 48 kJ, which has been determined for the BChl *d* dimer at above room temperature.[24]

On closer inspection, the situation appears to be more complicated for the (3^1S) epimer. In the intermediate temperature range (263−253 K) signals of various species coexist, and the spectrum of the dimers is encountered only at lower temperatures. These changes with temperature are fully reversible.

Upon cooling the signal intensity and integral of the (3^1S) epimer are significantly lowered, in contrast to the (3^1R) case. At the lowest temperature, the (3^1S) signals are about 4 times less intense than (3^1R). This cannot solely be due to signal broadening and splitting. In conjunction with the vis absorption data which show a parallel development upon the lowering of temperature it appears rather more likely that the population of the (3^1S) dimers decreases more rapidly than that of the (3^1R) dimers. The disappearance of the dimer signals is not accompanied by a growing-in of appropriate signals for the larger oligomers which are formed concurrently, as judged by their absorption at around 690 nm. The failure of ^{1}H-NMR spectroscopy to record the large oligomers must be due to their long correlation times.

Another indirect piece of evidence that larger aggregates do not give rise to detectable signals in the normal proton spectra is reflected by the fact that signals for a mixed dimer of (3^1R) and (3^1S) halves are not recorded in CD_2Cl_2: when CD_2Cl_2 solutions of the (3^1R) and (3^1S) epimers—each characterized by intense ^{1}H-NMR signals when separate in solution—are mixed, the signals practically disappear abruptly even at maximum instrumental sensitivity. This is explicable if the concurrent self-assembly of (3^1R) and (3^1S) epimers proceeds more readily than that of the separate (3^1R) and (3^1S) epimers. Large mixed aggregates composed of (3^1R) and (3^1S) monomer components, which are undetectable by solution ^{1}H-NMR, must therefore be formed selectively. It is of interest to note in this context that the low-temperature absorption spectra (not shown) of the ($R + S$) mixture do not yield any significant information on this point since the (3^1R) component spectrum covers any contribution by the much narrower (3^1S) bands.

Discussion

The results presented clearly suggest that a complex aggregation equilibrium is at work. High concentration, low temperature, and dilution by a nonpolar solvent shift this equilibrium toward larger self-assembled species. Scheme 1 shows the various species that we propose to play a role in the aggregation process.[27]

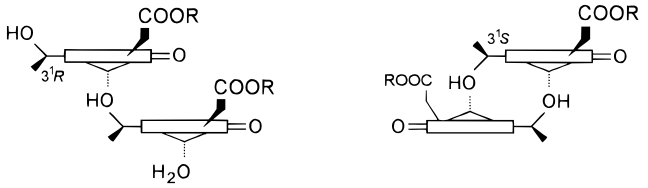

Figure 10. Schematic presentations of the most stable open [*anti*,*anti*-(3^1R)] and closed dimers [*anti*,*syn*-(3^1S)]; Δ, central zinc atom (the calculations were performed on fully 5-coordinated metal atoms;[12b] see text); *anti* and *syn* refer to the orientation of the propionyl ester group relative to the HO···Zn bond.

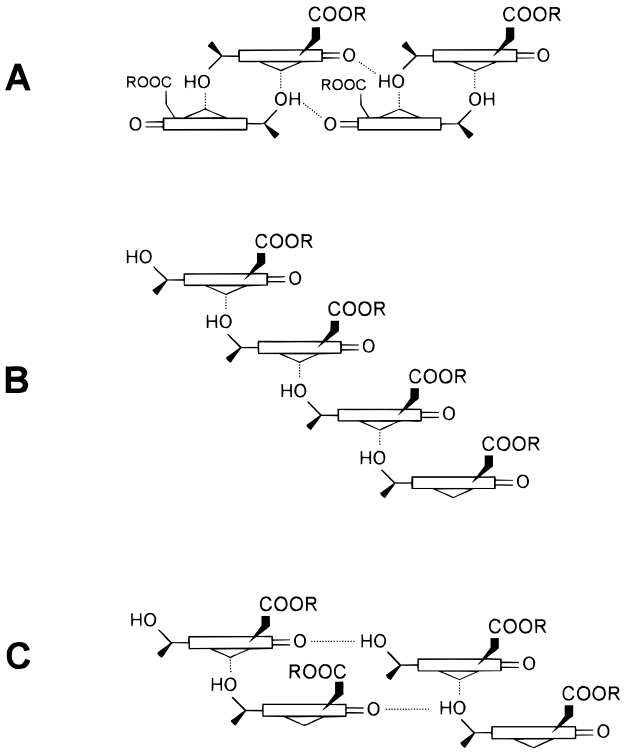

Figure 11. Schematic presentation of tetramers representing building blocks en route to type I and type II aggregates[17] (Δ, central metal atom). (A) Formed from closed dimers by >C═O···H−O hydrogen bonding; (B) from open dimers by HO···M ligation; (C) from open dimers by >C═O···H−O hydrogen bonding. A is a precursor of type I aggregates, B and C are precursors of type II.

A difficult problem is the distinction between open and closed dimers (Figure 10). Whereas two open dimers can associate to a tetramer by means of either another HO···Zn ligation or by >C═O···HO hydrogen bonding, two closed dimers can associate only through hydrogen bonding (Figure 11). Either of the alternative pathways for the open dimers can ultimately afford type II aggregates, whereas the formation of type I aggregates is the only option for closed dimers.[17,29] At present, the only means to estimate the preference in favor of one of the dimer structures are molecular mechanics calculations.[12b] While the exact parametrization of the force field remains questionable at this time, useful information may still be obtained as long as relative energies only are compared. Of the four possible open dimers, the *anti*,*anti* diastereoisomer is the most stable form. Closed dimers are higher in energy, which is the price to be paid for the second internal HO···Zn ligation. Nevertheless, the (3^1S) configurated *anti*,*syn* closed dimer may be populated somewhat as well since it presumably lies closest (albeit higher) in energy to the *anti*,*anti* isomer (for the magnesium analogs a difference of 17 kJ/mol has been calculated[12b]).

We ascribe to the (3^1R) species, which at high concentrations in CH_2Cl_2 is characterized by a 691-nm vis absorption maximum

and IR frequencies at 1651 cm^{-1} (a sharp ketone band)[11b] and in the 3150−3450 cm^{-1} region (broad hydroxyl bands), the >C═O···H-O···Zn network. This binding mode prevails also at low temperature. However, the differences in vis absorption maxima and carbonyl IR frequencies, and especially in the CD spectra, show that different aggregates of **1** are formed depending on whether the concentration or the temperature is changed. It is possible that the structural differences involved are of secondary nature only, the primary binding modes remaining the same under the changing conditions. Yet another different change in secondary structure occurs upon dilution of the CH_2Cl_2 solutions with hexane, as judged by the differences in vis absorption and CD between the CH_2Cl_2 and hexane samples and, in particular also, between the (3^1R) and (3^1S) epimers.

The greater overall complexity of the equilibrium in the case of the (3^1S) epimer in the initial solution phase can be attributed to the coexistence of open and closed dimers (see Scheme 1). The presence of several species is evident from the CD, IR, and vis absorption, as well as from the ^{1}H-NMR spectra at 263 and 253 K. Here, the signals do not simply coalesce as they do in the case of the (3^1R) epimer, whereas at still lower temperatures there remains only one set of split signals for a single species. Furthermore, a comparison of the low-temperature vis absorption spectra (Figure 2) reveals that in the (3^1R) sample the species absorbing at around 660 nm, which is attributed to dimers, is present at a higher concentration than the analog in the (3^1S) sample. In contrast to (3^1R)-**1**, most of the (3^1S) epimers at the low temperatures are evidently present in the more highly aggregated forms (with absorption maxima at 690 nm for (3^1R) and 696 nm for (3^1S), and neither detectable by ^{1}H-NMR; see results).

Two questions with regard to dimer reactivity remain open: (i) Do the nonsymmetrical open dimers (either epimer or both) detected by ^{1}H-NMR (Figure 9) serve as building blocks for the type II aggregates? On one hand, they may represent a small equilibrium fraction of the open dimers which, beyond reasonable doubt, do associate to type II. We should keep in mind, however, that the conformation of the dimeric type II precursors has not been determined independently. As an alternative possibility, on the other hand, the formation of the nonsymmetrical dimers may be irreversible, and they might not participate in any further association at all. It could thus be possible that there appear only ^{1}H-NMR signals of dimers which do not afford type II aggregates.

(ii) The second question concerns the structural factors that drive the equilibrium of a 1:1 mixture of (3^1R)- and (3^1S)-**1** more readily than that of the separate epimers toward higher aggregates. Neither molecular mechanics calculations nor spectroscopic information has so far provided any clues helping to interpret this observation.

As a final important aspect of the present investigation, the CD results deserve mention. The red shift and high intensity of the CD signals (Figures 4 and 5) for the higher aggregates, notably the type II aggregates, reflect strong excitonic interactions between the chromophores. The fact that the chlorosomes also exploit *in vivo* the tendency of the metallochlorins—bacteriochlorophylls *c* and *d* as well as the zinc models (**1**)—to combine *in vitro* strong excitonic coupling of the chromophores with a tubular arrangement at the supramolecular level suggests that this is an efficient way of optimizing the transfer of energy in the process of light energy harvesting.

Note Added in Proof. The effect of adventitious water on the monomer−dimers equilibria has been investigated in the case of (3^1R)-[Et,Et]BChl c_F in dichloromethane.[18] In the case of the zinc analogs **1**, water is also expected to drastically decrease the dimerization constant K_d.

Acknowledgment. We are indebted to Professor Volker Buss, University of Duisburg, for the offer to use his low-temperature CD equipment, and to Jörg Bitter, Marion Blumenthal, Gudrun Klihm, Shoichiro Takeuchi, and Manuela Trinoga for experimental assistance. Part of this work has been supported by Grants-in-Aid for Scientific Research (Nos. 05808052, 06808057) from the Japanese Ministry of Education, Science, Sports and Culture, Kato Memorial Bioscience Foundation, and Ritsumeikan Academic Research Grant for Overseas Joint Studies.

References and Notes

(1) See for examples of chlorophyll−protein complexes (LH2) of particularly intriguing structural beauty: McDermott, G.; Prince, S. M.; Freer, A. A.; Hawthornthwaite-Lawless, A. M.; Papiz, M. Z.; Cogdell, R. J.; Isaacs, N. W. *Nature* **1995**, *374*, 517−521. Koepke, J.; Hu, X.; Muenke, C.; Schulten, K.; Michel, H. *Structure* **1996**, *4*, 581−597.

(2) For reviews see: Tamiaki, H. *Coord. Chem. Rev.* **1996**, *148*, 183−197. Blankenship, R. E.; Olson, J. M.; Miller, M. In *Anoxygenic Photosynthetic Bacteria*; Blankenship, R. E.; Madigan, M. T., Bauer, C. E., Eds.; Kluwer Academic Publishers: Dordrecht, 1995; pp 399−435.

(3) Holzwarth, A. R.; Griebenow, K.; Schaffner, K. *Z. Naturforsch.* **1990**, *45c*, 203−206. Griebenow, K.; Holzwarth, A. R.; Schaffner, K. *Ibid.* 823−828. Holzwarth, A. R.; Griebenow, K.; Schaffner K. *J. Photochem. Photobiol. A: Chem.* **1992**, *65*, 61−71.

(4) Lawrence, D. S.; Jiang, T.; Levett, M. *Chem. Rev.* **1995**, *95*, 2229−2260. Philp, D.; Stoddart, J. F. *Angew. Chem.* **1996**, *108*, 1242−1286; *Angew. Chem., Int. Ed. Engl.* **1996**, *35*, 1154−1196.

(5) (a) Bystrova, M. I.; Mal'gosheva, I. N.; Kraskovskii, A. A. *Mol. Biol. Engl. Trans.* **1979**, *13*, 440−451. (b) Smith, K. M.; Kehres, L. A.; Fajer, J. *J. Am. Chem. Soc.* **1983**, *105*, 1387−1389. (c) Brune, D. C.; Nozawa, T.; Blankenship, R. E. *Biochemistry* **1987**, *26*, 8644−8652.

(6) Schaffner, K.; Braslavsky, S. E.; Holzwarth, A. R. In *Frontiers in Supramolecular Organic Chemistry and Photochemistry*; Schneider, H.-J., Dürr, Eds.; VCH Verlagsgemeinschaft mbH: Weinheim, 1991; pp 421−452.

(7) Tamiaki, H.; Miyatake, T.; Tanikaga, R.; Holzwarth, A. R.; Schaffner, K. *Angew. Chem.* **1996**, *108*, 810−812; *Angew. Chem., Int. Ed. Engl.* **1996**, *35*, 772−774.

(8) Chiefari, J.; Griebenow, K.; Fages, F.; Griebenow, N.; Balaban, T. S.; Holzwarth, A. R.; Schaffner, K. *J. Phys. Chem.* **1995**, *99*, 1357−1365.

(9) (a) Hildebrandt, Griebenow, K.; Holzwarth, A. R.; Schaffner, K. *Z. Naturforsch.* **1991**, *46c*, 228−232. (b) Hildebrandt, P.; Tamiaki, H.; Holzwarth, A. R.; Schaffner, K. *J. Phys. Chem.* **1994**, *98*, 2192−2197.

(10) Balaban, T. S.; Holzwarth, A. R.; Schaffner, K.; Boender, G.-J.; de Groot, H. J. M. *Biochemistry* **1995**, *34*, 15259−15266.

(11) For modifications of the nature and the positions of these functional groups see: (a) Tamiaki, H.; Holzwarth, A. R.; Schaffner, K. *J. Photochem. Photobiol. B: Biol.* **1992**, *15*, 355−360. (b) Tamiaki, H.; Amakawa, M.; Shimono, Y.; Tanikaga, R.; Holzwarth, A. R.; Schaffner, K. *Photochem. Photobiol.* **1996**, *63*, 92−99. (c) Tamiaki, H.; Holzwarth, A. R.; Schaffner, K. *Photosynth. Res.* **1994**, *41*, 245−251. (d) Jesorka, A.; Balaban, T. S.; Holzwarth, A. R.; Schaffner, K. *Angew. Chem.* **1996**, *108*, 3019−3021; *Angew. Chem., Int. Ed. Engl.* **1996**, *35*, 2861−2863. (e) Tamiaki, H.; Kubota, T.; Tanikaga, R. *Chem. Lett.* **1996**, 639−640. (f) Tamiaki, H.; Shimono, Y.; Rattray, A. G. M.; Tanikaga, R. *Bioorg. Med. Chem. Lett.* **1996**, *6*, 2085−2086. (g) Tamiaki, H.; Miyata, S.; Kureishi, Y.; Tanikaga, R. *Tetrahedron* **1996**, *52*, 12421−12432.

(12) (a) Holzwarth, A. R.; Schaffner, K. *Photosynth. Res.* **1994**, *41*, 225−233. (b) Balaban, T. S.; Holzwarth, A. R.; Schaffner, K. In preparation.

(13) The basics of bonding schemes of this type have initially been proposed by Smith et al.[5b] (*i.e.*, HO···M stacking) and Worcester et al. (C═O···H−O···M): Worcester, D. L.; Michalski, T. J.; Katz, J. J. *Proc. Natl. Acad. Sci. U.S.A.* **1986**, *83*, 3791−3795. They have been tentatively expanded later: Brune, D. C.; King, G. H.; Blankenship, R. E. In *Photosynthetic Light-harvesting Systems*; Scheer, H., Schneider, S., Eds.; Walter de Gruyter: Berlin, 1988; pp 141−151.

(14) In the chlorosomes[15] and *in vitro*[16] rod-shaped aggregates (type II[17]) of bacteriochlorophylls are encountered. Their macroscopic structure—inverted micellar tubes—has first been recognized experimentally by Katz and collaborators.[13,16]

(15) Staehelin, L. A.; Golecki, J. R.; Fuller, R. C.; Drews, G. *Arch. Mikrobiol.* **1978**, *119*, 269−277.

(16) Worcester, D. L.; Michalski, T. J.; Bowman, M. K.; Katz, J. J. *Mat. Res. Soc. Symp. Proc.* **1990**, *174*, 157−161.

(17) See ref 8 for the definition of type I and II BChl *c* aggregates, and ref 18 for the discussion of the corresponding scheme for BChl monomer−aggregate equilibria.

(18) Balaban, T. S.; Leitich, J.; Holzwarth, A. R.; Schaffner, K. To be submitted.

(19) A preliminary report on the diastereoselective control by the 3^1-hydroxy group of (3^1R)- and (3^1S)-**1** has already appeared.[20]

(20) Tamiaki, H.; Takeuchi, S.; Tanikaga, R.; Balaban, S. T.; Holzwarth, A. R.; Schaffner, K. *Chem. Lett.* **1994**, 401−402.

(21) Balaban, T. S.; Holzwarth, A. R.; Schaffner, K. *J. Mol. Struct.* **1995**, *349*, 183−186.

(22) Wakao, N.; Yokoi, N.; Isoyama, N.; Hiraiashi, A.; Shimada, K.; Kobayashi, M.; Kise, H.; Iwaki, M.; Itoh, S.; Takaichi, S.; Sakurai, Y. *Plant Cell Physiol.* **1996**, *37*, 889−893.

(23) Fujiwara, M.; Tasumi, M. *J. Phys. Chem.* **1986**, *90*, 5646−5650.

(24) Abraham, R. J.; Smith, K. M.; Goff, D. A.; Bobe, F. W. *J. Am. Chem. Soc.* **1985**, *107*, 1085−1087. Smith, K. M.; Bobe, F. W.; Goff, D. A.; Abraham, R. J. *Ibid.* **1986**, *108*, 1111−1120.

(25) *Closed* dimers have been defined[18] as arrangements, in which each 3^1-hydroxy group coordinates with the central metal atom of the opposite dimer half. In *open* dimers only one of the hydroxyls coordinates with the metal of the other half.

(26) A very recent ^{1}H-NMR study of [8Et,12Et]BChl c_F has shown, by intermolecular NOE, a nonsymmetrical *closed* dimer to occur at room temperature in chloroform containing a certain amount of methanol: Mizoguchi, T.; Limantara, L.; Matsuura, K.; Shimada, K.; Koyama, Y. *J. Mol. Struct.* **1996**, *379*, 249−265. This result is not at variance with our conclusions. Rather, it illustrates the diversity of aggregated species formed as a function of solvent nature, temperature, and concentration.

(27) Slightly simplified versions of Scheme 1 have been presented in refs 8 and 11c.

(28) A detailed assignment of the vis absorptions to the closed dimers and their oligomers appears premature at present.

(29) In the case of the closed dimers further oligomerization is restricted to a linear concatenation-like assembly affording type I (cf. Figure 11A). Type II aggregates[14] arise from open dimers by a combination of stack extension and stack pairing. The parent building blocks formed in these processes are exemplified in Figure 11 at the level of tetramers.